Systematic Genetic Analysis with Ordered Arrays of Yeast Deletion Mutants

Amy Hin Yan Tong, *et al.*

Science **294**, 2364 (2001);
DOI: 10.1126/science.1065810

viously expected (*18*, *19*). This also suggests that, in mammalian cells, initiation zones rather than individual origins may represent the functional units regulating DNA replication at the locus level.

Compared with other studies on DNA fibers (*16*, *20*–*23*), SMARD can provide qualitative and quantitative information about many aspects of DNA replication [supplementary table 1 (*5*)] and is potentially applicable to the study of endogenous loci in the mammalian genome.

References and Notes

1. J. L. Yates, in *DNA Replication in Eukaryotic Cells*, M. L. DePamphilis, Ed. (Cold Spring Harbor Laboratory, Plainview, NY, 1996), p. 751.
2. E. Kieff, in *Fields Virology*, B. N. Fields *et al.*, Eds. (Lippincott-Raven, Philadelphia, 1996), p. 2343.
3. J. L. Yates, N. Guan, *J. Virol.* **65**, 483 (1991).
4. R. D. Little, C. L Schildkraut, *Mol. Cell. Biol.* **15**, 2893 (1995).
5. Supplementary text (method), figures, and table are available on *Science* Online at www.sciencemag.org/cgi/content/full/294/5550/2361/DC1.
6. A. Bensimon, A. Simon, A. Chiffaudel, V. Croquette, F. Heslot, D. Bensimon *Science* **265**, 2096 (1994).
7. X. Michalet *et al.*, *Science* **277**, 1518 (1997).
8. J. F. Allemand, D. Bensimon, L. Jullien, A. Bensimon, V. Croquette, *Biophys. J.* **73**, 2064 (1997).
9. J. A. Aten, P. J. Bakker, J. Stap, G. A. Boschman, C. H. Veenhof, *Histochem. J.* **24**, 251 (1992).
10. J. W. Vaandrager *et al.*, *Blood* **88**, 1177 (1996).
11. R. J. Florijn *et al.*, *Hum. Mol. Genet.* **4**, 831 (1995).
12. P. Norio, C. L. Schildkraut, unpublished data.
13. J. P. Vaughn, P. A. Dijkwel, J. L. Hamlin, *Cell* **61**, 1075 (1990).
14. T. A. Gahn, C. L. Schildkraut, *Cell* **58**, 527 (1989).
15. V. Dhar, C. L. Schildkraut, *Mol. Cell. Biol.* **11**, 6268 (1991).
16. D. A. Jackson, A. Pombo, *J. Cell Biol.* **140**, 1285 (1998).
17. R. F. Kalejta, H. B. Lin, P. A. Dijkwel, J. L. Hamlin, *Mol. Cell. Biol.* **16**, 4923 (1996).
18. S. A. Greenfeder, C. S. Newlon, *Mol. Cell. Biol.* **12**, 4056 (1992).
19. A. M. Deshpande, C. S. Newlon, *Science* **272**, 1030 (1996).
20. J. A. Huberman, A. D. Riggs, *Proc. Natl. Acad. Sci. U.S.A.* **55**, 599 (1966).
21. J. A. Huberman, A. D. Riggs, *J. Mol. Biol.* **32**, 327 (1968).
22. J. Herrick, P. Stanislawski, O. Hyrien, A. Bensimon, *J. Mol. Biol.* **300**, 1133 (2000).
23. J. J. Blow, P. J. Gillespie, D. Francis, D. A. Jackson, *J. Cell Biol.* **152**, 15 (2001).
24. F. M. van de Rijke, R. J. Florijn, H. J. Tanke, A. K. Raap, *J. Histochem. Cytochem.* **48**, 743 (2000).
25. I. Parra, B. Windle, *Nature Genet.* **5**, 17 (1993).

26. We thank D. Dimitrova, R. Florijn, D. Schwartz, and B. Windle for advice during the development of SMARD; F. Camia and G. Mazzeo for advice on the analysis of the data; E. Bouhassira, J. Greally, J. A. Huberman, and J. Yates for helpful discussions and critical reading of the manuscript; and S. M. Shenoy and the Albert Einstein College of Medicine analytical imaging facility for technical support. This work was supported by NIH grants GM45751. Support was also provided by Cancer Center Support Grant NIH/NCI P30CA13330.

20 July 2001; accepted 6 November 2001

Systematic Genetic Analysis with Ordered Arrays of Yeast Deletion Mutants

Amy Hin Yan Tong,[1,2] Marie Evangelista,[3] Ainslie B. Parsons,[1,2] Hong Xu,[1,2] Gary D. Bader,[4,5] Nicholas Pagé,[6] Mark Robinson,[1] Sasan Raghibizadeh,[7] Christopher W. V. Hogue,[4,5] Howard Bussey,[6] Brenda Andrews,[2]* Mike Tyers,[2,5]* Charles Boone[1,2,3]*

In *Saccharomyces cerevisiae*, more than 80% of the ~6200 predicted genes are nonessential, implying that the genome is buffered from the phenotypic consequences of genetic perturbation. To evaluate function, we developed a method for systematic construction of double mutants, termed synthetic genetic array (SGA) analysis, in which a query mutation is crossed to an array of ~4700 deletion mutants. Inviable double-mutant meiotic progeny identify functional relationships between genes. SGA analysis of genes with roles in cytoskeletal organization (*BNI1*, *ARP2*, *ARC40*, *BIM1*), DNA synthesis and repair (*SGS1*, *RAD27*), or uncharacterized functions (*BBC1*, *NBP2*) generated a network of 291 interactions among 204 genes. Systematic application of this approach should produce a global map of gene function.

For *S. cerevisiae* deletion mutations have been constructed for all ~6200 known or suspected genes, identifying ~1100 essential yeast genes and resulting in 5100 viable haploid gene-deletion mutants, with over 30% of the genes remaining functionally unclassified (*1*). These findings highlight the capacity of yeast cells to tolerate deletion of a substantial number of individual genes, perhaps reflecting the molecular mechanisms that evolved to buffer the phenotypic consequences of genetic variation (*2*, *3*). Due to the high degree of genetic redundancy in yeast, the functions of thousands of yeast genes remain obscure.

Redundant functions can often be uncovered by synthetic genetic interactions, usually identified when a specific mutant is screened for second-site mutations that either suppress or enhance the original phenotype. In particular, two genes show a "synthetic lethal" interaction if the combination of two mutations, neither by itself lethal, causes cell death (*4*, *5*). Synthetic lethal relationships may occur for genes acting in a single biochemical pathway or for genes within two distinct pathways if one process functionally compensates for or buffers the defects in the other (*2*). Synthetic lethal screens have been used to identify genes involved in cell polarity, secretion, DNA repair, and numerous other processes (*6*–*9*). Despite the utility of this approach, just one or two different interactions are typically identified in a single screen (*2*). Saturation is rarely achieved presumably because some genes are refractory to forward mutagenesis and because subsequent analysis of synthetic lethal mutations and gene cloning is limited by practical constraints.

To enable high-throughput synthetic lethal analysis, we assembled an ordered array of ~4700 viable yeast gene-deletion mutants (*1*) and developed a series of pinning procedures in which mating and meiotic recombination are used to generate haploid double mutants (Fig. 1). A query mutation is first introduced into a haploid starting strain, of mating type *MAT*α, and then crossed to the array of gene-deletion mutants of the opposite mating type, *MAT***a**. Sporulation of resultant diploid cells leads to the formation of double-mutant meiotic progeny. The *MAT*α starting strain carries a reporter, *MFA1pr-HIS3*, that is only expressed in *MAT***a** cells and allows for germination of *MAT***a** meiotic progeny (*10*), which ensures that carryover of the diploid parental strain and/or conjugation of meiotic progeny does not give rise to false-negative interactions. Both the query mutation and the gene-deletion mutations were linked to dominant selectable markers to allow for selection of double mutants. Final pinning results in an ordered array of

[1]Banting and Best Department of Medical Research, University of Toronto, Toronto ON, Canada M5G 1L6. [2]Department of Medical Genetics and Microbiology, University of Toronto, Toronto ON, Canada M5S 1A8. [3]Biology Department, Queens University, Kingston ON, Canada K7L 3N6. [4]Department of Biochemistry, University of Toronto, Toronto ON, Canada M5S 1A8. [5]Program in Molecular Biology and Cancer, Samuel Lunenfeld Research Institute, Mt. Sinai Hospital, Toronto ON, Canada M5G 1X5. [6]Department of Biology, McGill University, Montreal PQ, Canada H3A 1B1. [7]Virtek Engineering Sciences, Inc. (VESI), 1 Bedford Road, Toronto ON, Canada M5R 2J7.

*To whom correspondence should be addressed. E-mail: brenda.andrews@utoronto.ca, tyers@mshri.on.ca, and charlie.boone@utoronto.ca

double-mutant haploid strains whose growth rate is monitored by visual inspection or image analysis of colony size. We refer to this procedure as synthetic genetic array (SGA) analysis.

To demonstrate proof of concept for SGA analysis, we tested a deletion of the *BNI1* gene (*bni1*Δ) against a test array of gene-deletion mutants including *bnr1*Δ, a known synthetic lethal with *bni1*Δ (*11*) (Fig. 2A). *BNI1* and *BNR1* both encode members of the highly conserved formin family and control the assembly of actin cables, which guide myosin motors that coordinate polarized cell growth and spindle orientation (*12*). As anticipated, the double-mutant cells at the *bnr1*Δ positions failed to grow, forming a residual colony with a reduced size relative to that of the control. Because the resultant double mutants are created by meiotic recombination, gene deletions that are genetically linked to the query mutation form double mutants at a reduced frequency; moreover, when the query mutation is identical to one of the gene deletions within the array, double mutants cannot form. Thus, cells at the *bni1*Δ position failed to grow under double-mutant selection. Even within the limited subset of genes in this pilot experiment, we detected previously unknown synthetic genetic interactions between *bni1*Δ and gene deletions of *CLA4* and *BUD6* (*AIP3*) (Fig. 2A). Cla4 is a kinase involved in actin patch assembly and regulation of the cell cycle–dependent transition from apical to isotropic bud growth (*13*, *14*); Bud6 forms a complex with Bni1 and actin to control actin cable assembly and cell polarity (*15*). Tetrad analysis confirmed that both the *bni1*Δ *bnr1*Δ and *bni1*Δ *cla4*Δ double mutants were inviable and that the *bni1*Δ *bud6*Δ double mutant was associated with a slower growth rate or "synthetic sick" phenotype, reflecting reduced fitness of the double mutant relative to the respective single mutants (Fig. 2B).

We next screened a *bni1*Δ query strain against an array of 4672 different viable deletion strains. For high-throughput automated screening, we designed a robotic system for manipulation of high-density yeast arrays (*16*). To ensure reproducibility within a screen and to facilitate visual scoring, we arrayed the deletion strains in pairs, at 768 strains per plate. We scored 67 potential synthetic lethal/sick interactions, 51 (76%) of which were confirmed by tetrad analysis. At the current stage of development, SGA analysis yields a substantial number of false-positives; however, these can be reduced by repeated screening or removed through confirmation of the interactions by tetrad analysis, which is straightforward because the tetrads can be obtained directly from the array of sporulated diploids (*17*). To group the identified genes by function, we assembled a list of their cellular roles as defined by the Yeast Proteome Database (YPD) (*18*). The *BNI1* interactions were highly enriched for genes with roles in cell polarity (20%), cell wall maintenance (18%), and mitosis (16%). Pathways critical for the fitness of *bni1*Δ cells were revealed by multiple interactions with subsets of genes involved in bud emergence (*BEM1*, *BEM2*, and *BEM4*), chitin synthase III activity (*CHS3*, *SKT5*, *CHS5*, *CHS7*, and *BNI4*), mitogen-activated protein (MAP) kinase pathway signaling (*BCK1* and *SLT2*), the cell cycle–dependent transition from apical to isotropic bud growth (*CLA4*, *ELM1*, *GIN4*, and *NAP1*), and the dynein/dynactin spindle orientation pathway (*DYN1*, *DYN2*, *PAC1*, *PAC11*, *ARP1*, *JNM1*, *NIP100*). We identified 8 of the 11 previously known *bni1*Δ synthetic lethal/sick interactions (*BNR1*, *SLT2*, *BCK1*, *DYN1*, *ARP1*, *PAC1*, *NIP100*, *ASE1*) (*18*). Of the three that were not identified, *CDC12* and *PKC1* are not contained in our deletion set, whereas cells lacking *HOF1* grow very slowly and are apparently beyond the sensitivity of the assay (*17*). In total, we discovered 43 previously unknown synthetic genetic interactions for *bni1*Δ, including 9 genes of unclassified function.

Because genetic interactions can be represented as binary gene-gene relationships, multiple SGA screens should generate a network of genetic interactions that depicts

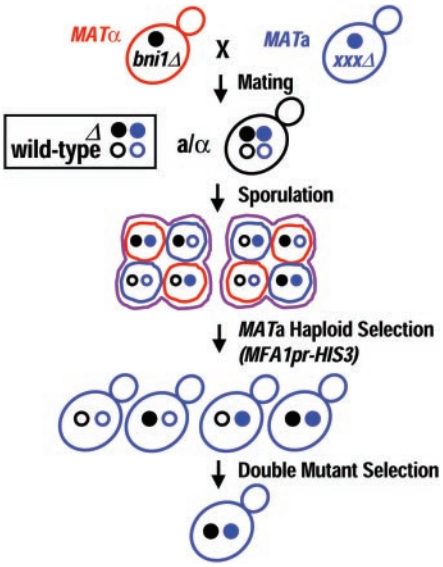

Fig. 1. Synthetic genetic array methodology (*16*). (i) A *MAT*α strain carrying a query mutation (*bni1*Δ) linked to a dominant selectable marker, such as the nourseothricin-resistance marker *natMX* that confers resistance to the antibiotic nourseothricin, and an *MFA1pr-HIS3* reporter is crossed to an ordered array of *MAT***a** viable yeast deletion mutants, each carrying a gene deletion mutation linked to a kanamycin-resistance marker (*kanMX*). Growth of resultant heterozygous diploids is selected for on medium containing nourseothricin and kanamycin. (ii) The heterozygous diploids are transferred to medium with reduced levels of carbon and nitrogen to induce sporulation and the formation of haploid meiotic spore progeny. (iii) Spores are transferred to synthetic medium lacking histidine, which allows for selective germination of *MAT***a** meiotic progeny because these cells express the *MFA1pr-HIS3* reporter specifically. (iv) The *MAT***a** meiotic progeny are transferred to medium that contains both nourseothricin and kanamycin, which then selects for growth of double-mutant meiotic progeny.

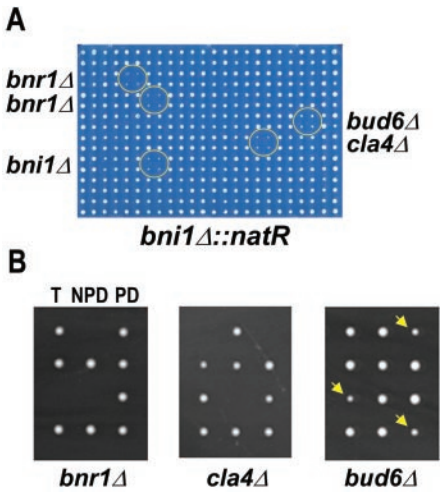

Fig. 2. Final double-mutant array and tetrad analysis for SGA synthetic lethal analysis with *bni1*Δ and a test array (*16*). (**A**) *bni1*Δ*::natR* cells were crossed to a test array containing 96 deletion mutants, each arrayed in quadruplicate in a square pattern. *bnr1*Δ was duplicated within the array. The final array that selects for growth of the *bni1*Δ double mutants is shown. Synthetic lethal/sick interactions lead to the formation of residual colonies (yellow circles) that were relatively smaller than the equivalent colony on the wild-type control plate. Synthetic lethal/sick interactions were scored with *bnr1*Δ, *cla4*Δ, and *bud6*Δ. When the query mutation was identical to one of the gene deletions within the array, double mutants could not form because haploids carry a single copy of each allele; therefore, *bni1*Δ appeared synthetic lethal with itself. (**B**) Tetrad analysis of meiotic progeny derived from diploid cells heterozygous for *bni1*Δ and either *bnr1*Δ, *cla4*Δ, or *bud6*Δ. Tetratypes (T) contain one double-mutant spore; nonparental ditypes (NPD) contain two double-mutant spores; and parental ditypes (PD) lack double-mutant spores. The spores were micromanipulated onto distinct positions on the surface of agar medium and then allowed to germinate to form a colony. *bni1*Δ *bnr1*Δ and *bni1*Δ *cla4*Δ double mutants are inviable and therefore fail to form a colony, whereas *bni1*Δ *bud6*Δ double mutants showed a synthetic slow growth (sick) phenotype (yellow arrows). The genetic make-up of the double mutants was inferred by replica plating the colonies to medium containing nourseothricin, which selects for growth of *bni1*Δ*::natR* cells, and kanamycin, which selects for growth of the *bnr1*Δ, *cla4*Δ, and *bud6*Δ gene-deletion mutants.

the functional relationships between genes and pathways. The SGA synthetic lethal data set was first imported into the Biomolecular Interaction Network Database (BIND) (*19*), then formatted with BIND tools (*16*) and exported to the Pajek package (*20*), a program originally designed for the graphical analysis of social interactions. The network shown in Fig. 3 contains the interactions observed for *BNI1* and those for seven other query genes, *BBC1* (*MTI1*), *ARC40*, *ARP2*, *BIM1*, *NBP2*, *SGS1*, and *RAD27*, as described below. The network contains 204 genes, represented as nodes on the graph, and 291 genetic interactions, represented as edges connecting the genes. To visualize subsets of functionally related genes, we color-coded the genes according to their YPD cellular roles and aligned them with one another on the basis of their roles and connectivity (*16*). The function of the genes with unknown cellular roles (colored black) is predicted by the roles of surrounding genes that show a similar connectivity.

If these interactions identify functionally related genes, then some of the uncharacterized genes from the *bni1*Δ screen should also participate in cortical actin assembly or spindle orientation. To test this, we conducted an SGA screen using a strain deleted for a previously uncharacterized gene, *BBC1*, which leads to a synthetic sick phenotype in combination with *bni1*Δ. We scored 17 potential synthetic lethal/sick interactions for *bbc1*Δ, most of which have YPD-classified cell polarity or cell structure (cytoskeletal) roles (Fig. 3). In particular, *bbc1*Δ showed interactions with several genes whose products control actin polymerization and localize to cortical actin patches (*CAP1*, *CAP2*, *SAC6*, and *SLA1*), suggesting that *BBC1* may be involved in assembly of actin patches or their dependent processes. Further experiments demonstrated that Bbc1 localized predominantly to cortical actin patches and binds to Las17 (Bee1), a member of the WASp (Wiskott-Aldrich Syndrome protein) family proteins that controls the assembly of cortical actin patches through regulation of the Arp2/3 actin nucleation complex (*21*, *22*).

We next focused on *ARC40* and *ARP2*, both of which encode subunits of the Arp2/3 complex (*23*), a major regulator of actin nucleation, the rate-limiting step for actin polymerization. Because *ARC40* is an essential gene, we first isolated a temperature-sensitive conditional lethal allele, *arc40-40*, by polymerase chain reaction (PCR) mutagenesis and then conducted the screen at a tempera-

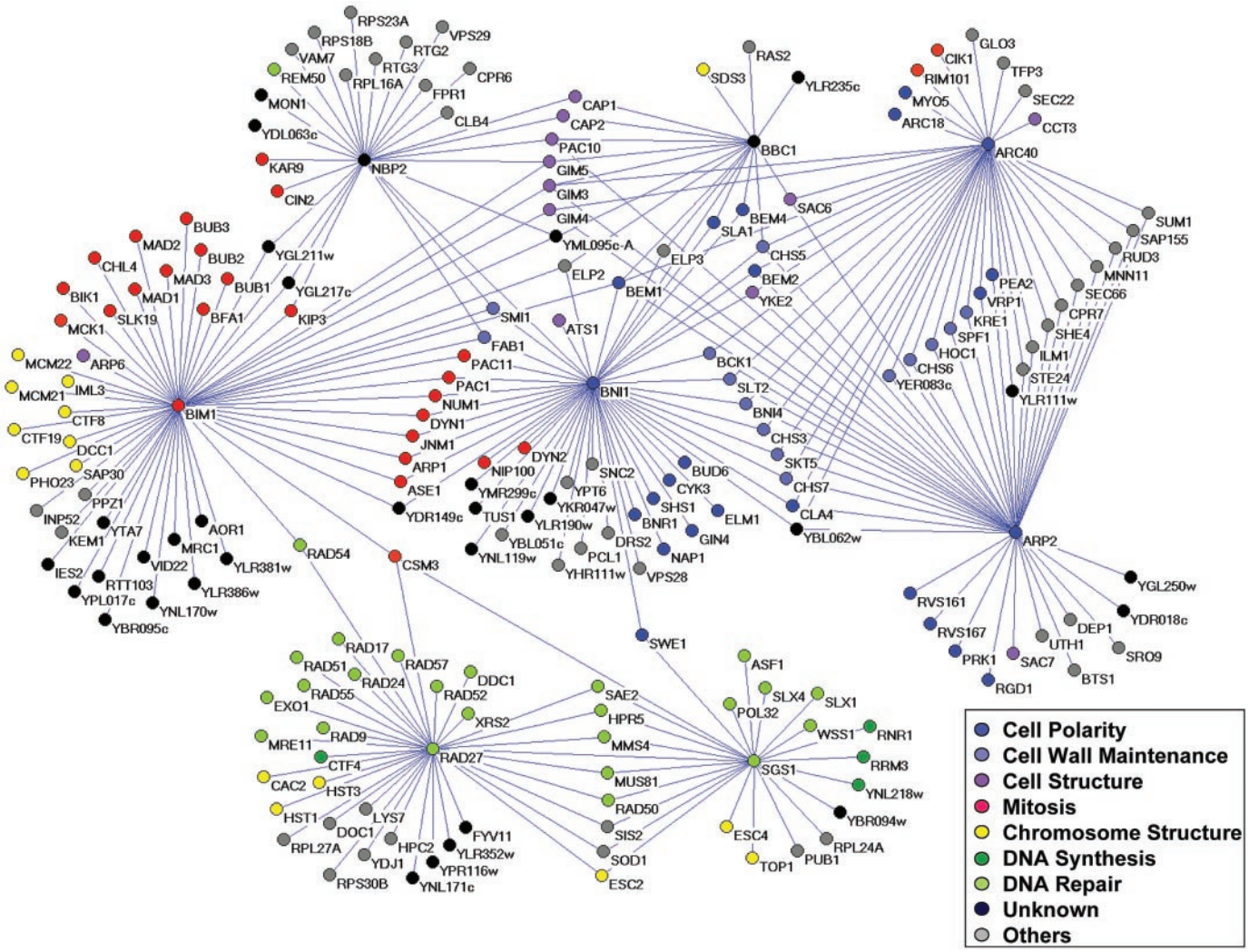

Fig. 3. Genetic interaction network representing the synthetic lethal/sick interactions determined by SGA analysis. Genes are represented as nodes, and interactions are represented as edges that connect the nodes; 291 interactions and 204 genes are shown. All of the interactions were confirmed by tetrad analysis, with 8 to 14 tetrads examined in each case. The genes are colored according to their YPD cellular roles (*18*). For genes assigned multiple cellular roles, we chose one that we considered the most probable on the basis of a review of published abstracts for studies concerning the gene. Synthetic lethal relationships can also be represented by two-dimensional hierarchical clustering, as is used for analysis of DNA microarray experiments (*16*).

ture that was semipermissive for growth. We scored 40 synthetic lethal/sick interactions for *arc40-40* (Fig. 3), most of which have cell polarity or cell wall maintenance roles, including two genes involved in Arp2/3 activation (*VRP1* and *MYO5*). From a similar screen with a temperature-sensitive *ARP2* allele, *arp2-33*, we scored a total of 44 synthetic lethal/sick interactions. The *ARP2* screen identified 31 interactions that were shared with *ARC40* (Fig. 3). Both screens identified a relatively small number of unique interactions, which included genes implicated in actin patch assembly (*MYO5* and *ARC18* with *arc40-40* but not *arp2-33*; *PRK1* with *arp2-33* but not *arc40-40*), and may reflect roles specific to each Arp2/3 subunit (*23*, *24*).

Bim1 determines spindle orientation through physical interactions with cytoplasmic microtubules and with Kar9, which marks the microtubule capture site at the bud cortex (*25*). With a *BIM1* gene deletion as the query, we scored a total of 56 genetic interactions by SGA synthetic lethal analysis (Fig. 3). Many of the *BIM1* interactions occurred with mitotic genes, including multiple genes involved in nuclear migration and spindle orientation during mitosis (*BIK1*, *SLK19*, *KIP3*, *PAC11*, *PAC1*, *NUM1*, *DYN1*, *JNM1*, *ARP1*, *ASE1*), and with several genes encoding components of the Bub2- and Mad2-dependent spindle-assembly checkpoints (*BUB1*, *BUB2*, *BUB3*, *BFA1*, *MAD1*, *MAD2*, and *MAD3*). *BIM1* also interacted with a group of genes assigned a chromatin/chromosome structure cellular role, many of which have been implicated in kinetochore function (*CTF8*, *CTF19*, *MCM21*, *MCM22*, *CHL4*), and with *ARP6*, a gene encoding a nuclear-localized actin-related protein of unknown function. The interactions with spindle-assembly checkpoint and kinetochore genes suggests that Bim1 may participate in the attachment of microtubules to the kinetochore, a possibility supported by a two-hybrid interaction with the kinetochore component Duo1 (*18*). A total of 16 genes with unclassified cellular roles interacted with *BIM1*. To examine one of the uncharacterized genes in more detail, we conducted an SGA analysis of a deletion of *NBP2*, which revealed interactions with several genes involved in nuclear migration and spindle function (*KAR9*, *CIN2*, *KIP3*), actin assembly (*CAP1*, *CAP2*), and the de novo folding of actin and tubulin (*PAC10*, *GIM5*) (Fig. 3), suggesting a general role for Nbp2 in cytoskeletal organization.

To explore the potential for SGA methodology to identify interactions for genes with roles distinct from cytoskeletal organization and cell polarity, we undertook screens with two nonessential genes, *SGS1* and *RAD27*. *SGS1* encodes the yeast homolog of the human Werner's syndrome protein, WRN, a member of the RecQ family of DNA helicases (*9*), whereas *RAD27* encodes an enzyme that processes Okazaki fragments during DNA synthesis and repair (*26*). SGA analysis identified 24 synthetic interactions for *SGS1* and 36 synthetic interactions for *RAD27*, most of which involve genes with cellular roles in DNA synthesis and repair (Fig. 3).

One of the caveats of the SGA method is the absence of essential genes from the genomewide arrays. This drawback could be solved by construction of a complete set of marked conditional mutations in essential genes. It is straightforward to extend SGA analysis to multiple gene interactions, by beginning with a multiple mutant starting strain; for example, by beginning with a double-mutant query strain, arrays of triple mutants can be selected with the SGA protocol. Arrays of yeast cells each carrying an open reading frame on a high-copy plasmid or under high-level conditional expression will allow comprehensive dosage suppression and synthetic dosage lethality screens (*27*), which could be performed with yeast genes or heterologous genes. To facilitate conventional forward genetic approaches, the marked gene deletions can be used to systematically map both recessive and dominant mutations, and potentially multigenic traits, that lead to a gain-of-function phenotype (*28*). In theory, SGA methodology should also allow us to backcross the entire set of deletion mutations into another genetic background to analyze strain-specific traits (*28*). The high-density arrays in SGA screens should also permit efficient detection of chemical-genetic interactions on medium containing a compound of interest (*29*). The unique oligonucleotide "bar code" tags built into each deletion strain may be exploited for quantitative analysis of growth phenotypes by hybridization of pooled SGA colonies to DNA microarrays of bar code sequences (*30*). Each of these variations can be tailored to high-throughput analysis of specific pathways by use of mini-arrays of defined composition, as derived from initial genomewide surveys.

By extrapolation of the results presented here, we estimate that on the order of 300 SGA screens covering judiciously selected query genes will provide an effective working genetic scaffold, which should reveal many of the molecular mechanisms behind genetic robustness and buffering (*2*, *3*). Because gene function is often highly conserved, a comprehensive functional genetic map of *S. cerevisiae* will provide a template to understand the relationships among analogous pathways in metazoans. With the advent of systematic genetic-perturbation methodologies, such as large-scale RNA interference analysis of gene function in *Caenorhabditis elegans* (*31*), the SGA approach is in principle applicable to metazoan systems.

References and Notes

1. E. A. Winzeler *et al.*, *Science* **285**, 901 (1999).
2. J. L. Hartman IV, B. Garvik, L. Hartwell, *Science* **291**, 1001 (2001).
3. A. Wagner *Nature Genet.* **24**, 355 (2000).
4. P. Novick, B. C. Osmond, D. Botstein, *Genetics* **121**, 659 (1989).
5. L. Guarente, *Trends Genet.* **9**, 362 (1993).
6. A. Bender A, J. R. Pringle, *Mol. Cell. Biol.* **11**, 1295 (1991).
7. T. Wang, A. Bretscher, *Genetics* **147**, 1595 (1997).
8. C. Y. Chen, T. R. Graham, *Genetics* **150**, 577 (1998).
9. J. R. Mullen, V. Kaliraman, S. S. Ibrahim, S. J. Brill, *Genetics* **157**, 103 (2001).
10. I. Herskowitz, J. Rine, J. Strathern, in *The Molecular and Cellular Biology of the Yeast* Saccharomyces cerevisiae, vol. 2, *Gene Expression*, E. W. Jones, J. R. Pringle, J. R. Broach, Eds. (Cold Spring Harbor Laboratory, Cold Spring Harbor, NY, 1992), pp. 583–656.
11. T. Kamei *et al.*, *J. Biol. Chem.* **273**, 28341 (1998).
12. M. Evangelista *et al.*, *Nature Cell Biol.*, in press.
13. H. Tjandra, J. Compton, D. Kellogg, *Curr. Biol.* **8**, 991 (1998).
14. M. S. Longtine *et al.*, *Mol. Cell. Biol.* **20**, 4049 (2000).
15. M. Evangelista *et al.*, *Science* **276**, 118 (1997).
16. The following supplementary material is available on *Science* Online at www.sciencemag.org/cgi/content/full/294/5550/2364/DC1: supplementary table 1, a table of the deletion mutants used to create the double-mutant arrays shown in Fig. 2A by SGA analysis; supplementary table 2, a table of the 4672 unique deletion mutants assembled for large-scale SGA analysis; supplementary notes, a description of the materials and methods for SGA analysis and bioinformatic analysis (yeast strains will be provided upon request); supplementary table 3, a table summarizing all the synthetic lethal/fitness interactions; supplementary table 4, a table of 523 gene deletions within the array that often appeared to be synthetically lethal with a wild-type control strain; supplementary table 5, a table of the overlap of the genetic interactions presented in Fig. 3 and the published genetic interactions assembled at MIPS (Munich Information Center for Protein Sequences) and YPD; supplementary fig. 1, a figure of the protein-protein interactions corresponding to genes within the genetic-interaction network shown in Fig. 3; supplementary table 6, a table of the gene deletions that are linked to the query gene and appeared to be synthetically lethal; supplementary fig. 2, a figure that shows two-dimensional clustering analysis of synthetic lethal interactions; supplementary table 7, a table that shows an analysis of the false-positives for the *BIM1* and *SGS1* screens as a comparison of the list of gene deletions that were scored as positive by SGA analysis to the list of gene deletions that were ultimately confirmed to be synthetically lethal by tetrad analysis; and supplementary table 8, a table of the synthetic genetic interactions and their BIND identification numbers.
17. As assessed by tetrad dissection, the method is subject to ~20 to 50% false-positive interactions, depending upon the number of times a particular screen has been repeated (*16*). False-positives may reflect the greater stringency of growth conditions used for double mutants in the array context (high density on minimal medium) than in standard tetrad analysis (low density on rich medium). In particular, because the SGA method relies on bulk transfer of double-mutant progeny, mutations that lower sporulation or germination efficiency below a certain threshold may incorrectly score as inviable. Additional unmarked genetic alterations, such as the aneuploidy that is associated with some of the deletion mutants (*32*), may also contribute to the incidence of false-positives. Because SGA analysis generates a large number of synthetic lethal interactions relative to those generated by traditional methods, it is difficult to assess false-negatives; however, for the query mutations reported here, SGA analysis identified almost all (~92%) previously known interactions associated with the viable deletion mutants (*16*).
18. References for all the genes mentioned in this study can be found at YPD (www.proteome.com/), the *Saccharomyces* Genome Database (SGD) (http://genome-www.stanford.edu/Saccharomyces/), and

MIPS (www.mips.biochem.mpg.de/). Yeast genetic and protein-interaction data sets were obtained from YPD and MIPS databases. Cellular role and biochemical functions were obtained from YPD.
19. G. D. Bader *et al.*, *Nucleic Acids Res.* **29**, 242 (2001); www.bind.ca.
20. http://vlado.fmf.uni-lj.si/pub/networks/pajek/.
21. A. H. Y. Tong *et al.*, *Science*, in preparation.
22. Because both Bbc1 (Mti1) and Vrp1 bind yeast type I myosins (Myo3 and Myo5), and a *BBC1* deletion mutation (*bbc1*Δ) suppresses the temperature sensitivity and endocytosis defects of *vrp1* mutants, Bbc1 and Vrp1 may antagonistically control the function of type I myosins (*33*).
23. D. C . Winter, E. Y. Choe, R. Li, *Proc. Natl. Acad. Sci. U.S.A.* **96**, 7288 (1999).
24. M. J. Cope, S. Yang, C. Shang, D. G. Drubin, *J. Cell Biol.* **144**, 1203 (1999).
25. K. Bloom, *Nature Cell Biol.* **2**, E96 (2000).
26. H. Debrauwere, S. Loeillet, W. Lin, J. Lopes, A. Nicolas, *Proc. Natl. Acad. Sci. U.S.A.* **98**, 8263 (2001).
27. E. S. Kroll, K. M. Hyland, P. Hieter, J. J. Li, *Genetics* **143**, 95 (1996).
28. Because double mutants are created by meiotic crossover, a set of gene deletions that are linked to the query gene, which we refer to as the "linkage group," form double mutants at reduced frequency. For example, the gene-deletion mutations of 13 different genes that are linked to *BNI1* and contained on the array [*YNL253W*, *YNL254C*, *YNL255C*, *YNL257C*, *YNL259C*, *YNL264C*, *YNL265C*, *YNL266W*, *YNL268W*, *YNL270W*, *BNI1* (*YNL271W*), *YNL273W*, and *YNL275W*] appeared to be synthetically lethal with the *bni1*Δ query mutation. A list of the gene deletions that were linked to the query gene and appeared to be synthetically lethal with the query gene is provided as supplementary material (*16*). Thus, systematic random spore analysis with the set of gene-deletion mutants provides a method for genetically mapping mutations that are linked to a dominant selectable marker. Similarly, alleles that are associated with a gain-of-function phenotype can also be mapped. For example, through identification of linkage groups that are defective for the gain-of-function phenotype, we should be able to map mutations that result in filamentous growth or high-temperature growth, neither of which are associated with the S288C strains within the deletion array, or suppressors of the lethality associated with temperature-sensitive alleles linked to a dominant selectable marker.
29. L. H. Hartwell *et al.*, *Science* **278**, 1064 (1997).
30. Each of the deletion mutations is marked with two unique oligonucleotide bar codes that were integrated along with common flanking primer sites for PCR amplification (*34*). Because the bar codes allow the growth rate of all the deletion mutants to be followed within a population of cells, the steps for creating double mutants outlined in Fig. 1 could be carried out with a pool of deletion mutants. In this scheme, synthetic lethality or slow growth of the resulting double mutants would be analyzed by PCR amplification of the bar codes and subsequent hybridization to a bar-code microarray, such that the intensity of the signal observed for an element on the bar-code array reflects the representation of the double-mutant meiotic progeny (*35*). As another means of large-scale synthetic lethal analysis, a collection of deletion mutant strains can be transformed en masse with a gene-deletion cassette and the lethal double-mutant transformants predicted by bar-code microarray analysis (*36*).
31. R. Barstead, *Curr. Opin. Chem. Biol.* **5,** 63 (2001).
32. T. R. Hughes *et al.*, *Nature Genet.* **25**, 333 (2000).
33. J. Mochida, T. Yamamoto, K. Fujimura-Kamada, K. Tanaka, personal communication.
34. D. D. Shoemaker, D. A. Lashkari, D. Morris, M. Mittmann, R. W. Davis, *Nature Genet.* **14**, 450 (1996); www-sequence.stanford.edu/group/yeast_deletion_project/deletions3.html.
35. M. Maiolatesi, P. Bieganowski, D. Shoemaker, C. Brenner, personal communication.
36. S. L. Ooi, *et al.*, personal communication.
37. We thank B. Drees, S. Fields, and J. Friesen for advice on the robotic manipulation of yeast arrays; C. Udell for construction of the *MFA1pr-HIS3* reporter; P. Jorgensen for discussions concerning SGA mapping of gain-of-function mutations; and G. Brown, N. Davis, D. Durocher, S. Gasser, S. Fields, T. Hughes, and T. Roemer for comments on the manuscript. Supported by grants from the Canadian Institute of Health Research (B.A., C.B., C.H., and M.T.), an operating grant from the National Cancer Institute of Canada (C.B.), and an operating grant from the Natural Sciences and Engineering Research Council of Canada (H.B.).

28 August 2001; accepted 13 November 2001

Correction of Sickle Cell Disease in Transgenic Mouse Models by Gene Therapy

Robert Pawliuk,[1,2] Karen A. Westerman,[1,2] Mary E. Fabry,[3] Emmanuel Payen,[4] Robert Tighe,[1,2] Eric E. Bouhassira,[3] Seetharama A. Acharya,[3] James Ellis,[5] Irving M. London,[1,6] Connie J. Eaves,[7] R. Keith Humphries,[7] Yves Beuzard,[4] Ronald L. Nagel,[3] Philippe Leboulch,[1,2,4,8]*

Sickle cell disease (SCD) is caused by a single point mutation in the human β^A globin gene that results in the formation of an abnormal hemoglobin [HbS ($\alpha_2\beta^S{}_2$)]. We designed a β^A globin gene variant that prevents HbS polymerization and introduced it into a lentiviral vector we optimized for transfer to hematopoietic stem cells and gene expression in the adult red blood cell lineage. Long-term expression (up to 10 months) was achieved, without preselection, in all transplanted mice with erythroid-specific accumulation of the antisickling protein in up to 52% of total hemoglobin and 99% of circulating red blood cells. In two mouse SCD models, Berkeley and SAD, inhibition of red blood cell dehydration and sickling was achieved with correction of hematological parameters, splenomegaly, and prevention of the characteristic urine concentration defect.

Sickle cell disease (SCD) is one of the most prevalent autosomal recessive disorders worldwide. In 1957, SCD became the first genetic disorder for which a causative mutation was identified at the molecular level: the substitution of valine for glutamic acid in human β^A-globin codon 6 (*1*). In homozygotes, the abnormal hemoglobin (Hb) [HbS ($\alpha_2\beta^S{}_2$)] polymerizes in long fibers upon deoxygenation within red blood cells (RBCs), which become deformed ("sickled"), rigid, and adhesive, thereby triggering microcirculation occlusion, anemia, infarction, and organ damage (*2, 3*).

Human γ-globin is a strong inhibitor of HbS polymerization, in contrast to human β^A-globin, which is effective only at very high concentrations (*4*). Hence, gene therapy of SCD was proposed by means of forced expression of human γ-globin or γ/β hybrids in adult RBCs after gene transfer to hematopoietic stem cells (HSCs) (*5–11*).

Although the discovery of the human β-globin locus control region (LCR) held promise to achieve high globin gene expression levels (*12, 13*), the stable transfer of murine onco-retroviral vectors encompassing minimal core elements of the LCR proved especially challenging (*14–20*). To allow the transfer of larger LCR and globin gene sequences, we proposed the use of RNA splicing and export controlling elements that include the Rev/R responsive element (RRE) components of human immunodeficiency virus (HIV) (*21*), and an RRE-bearing HIV-based lentiviral vector recently resulted in substantial amelioration of β-thalassemia in transplanted mice (*22*). However, gene expression remained heterocellular, and the amount of human β^A-globin found incorporated in Hb tetramers in a nonthalassemic background is unlikely to be therapeutic for SCD (*22*). Here, a lentiviral vector was optimized to express an antisickling protein at therapeutic levels in virtually all circulating RBCs of SCD mouse models.

We constructed a human β^A-globin gene variant mutated at codon 87 to encode the amino-acid residue believed to be responsible

[1]Harvard-MIT, Division of Health Sciences and Technology, Massachusetts Institute of Technology, Cambridge, MA 02139, USA. [2]Genetix Pharmaceuticals, Cambridge, MA 02139, USA. [3]Division of Hematology, Albert Einstein College of Medicine, Bronx, NY 10461, USA. [4]INSERM EMI 0111, Hôpital Saint-Louis, 75010 Paris, France. [5]Department of Genetics, Hospital for Sick Children, Toronto, ON M5G1X8, Canada. [6]Department of Biology, Massachusetts Institute of Technology, Cambridge, MA 02139, USA. [7]The Terry Fox Laboratory and the University of British Columbia, Vancouver, BC V5Z3L6, Canada. [8]Harvard Medical School and Department of Medicine, Brigham and Women's Hospital, Boston, MA 02115 USA.

*To whom correspondence should be addressed. E-mail: pleboulch@mit.edu